



Chemical and electrochemical treatment effects on the morphology, structure, and electrochemical performance of carbon fiber with different graphitization indexes

D. A. L. Almeida¹ · A. B. Couto¹ · S. S. Oishi¹ · N. G. Ferreira¹

Received: 31 January 2018 / Revised: 26 June 2018 / Accepted: 27 June 2018 / Published online: 31 July 2018
© Springer-Verlag GmbH Germany, part of Springer Nature 2018

Abstract

The association of capacitive charging of the double-layer and a faradic redox reaction is desirable on carbon fiber (CF) when oxygen functional groups or other heteroatoms are present on its surface enhancing its capacitive properties. In this work, a systematic study of carbon fiber produced at three different heat treatment temperatures (HTT) of 1000, 1500, and 2000 °C was performed upon two approaches: middle (chemical) and severe (electrochemical) oxidative treatments. Morphological, structural, and surface chemical changes were investigated by field emission gun-scanning electron microscopy, X-ray diffraction, Raman spectroscopy, and X-ray photoelectron spectroscopy. Electrochemical responses were analyzed by galvanostatic charge/discharge, electrochemical impedance spectroscopy, and cyclic voltammetry. Raman results showed that the electrochemical oxidation promoted structural variation on CF samples independently of their HTT. Concerning the specific capacitance, the results indicated that chemical treatment was more effective for CF1000 than those for CF1500 and CF2000. This behavior may be attributed to higher amount of oxygen on its surface as well as its lower structural ordering. Otherwise, for CF1000, the electrochemical treatment increased its resistivity. However, for CF1500 and CF2000, which present higher graphitization levels and less heteroatom contents, greater capacitance values were observed after their electrochemical oxidative treatment.

Keywords Carbon fiber · Oxidative treatment · Supercapacitor

Introduction

The development of modern devices, which enables solutions for the global energy problem with less environmental impact, has been the subject of intense research. Nowadays, carbon-based materials have been used as electrodes for supercapacitors due to their physical and chemical properties. The electrical properties of supercapacitors are determined by the selection of electrode material [1]. Therefore, these devices require the search of new materials as electrodes with high efficiency.

Carbon fiber (CF) is well known by its lower density, high mechanical resistance, resistance to corrosion, and high temperatures [2, 3]. CF has multiple possibility applications ranging from reinforcement materials in composites to electrodes and supercapacitors [4, 5]. The CF offers the advantage of being used as electrode because it is not necessary any substrates or binders to improve its conductivity or electric contact [6, 7]. Besides, it allows a plausible strategy to maximize the energy density of supercapacitors [8]. In this context, CF is one of the most promising materials due to its high surface area and fast charge/discharge kinetics [9]. It is noteworthy that the double-layer charge storage is a surface process, and thus, it is greatly influenced by the CF surface characteristics [10]. Physical and chemical properties of carbon fiber surface can be affected by both heat temperature treatment (HTT) and oxidative treatment [4, 11, 12]. Regarding the CF HTT increase, the ordering and orientation of the crystallites in the direction of the fiber axis are improved. In addition, the CF morphology change as well as the removal of its surface heteroatoms can take place [11, 12]. Chemical and electrochemical oxidations are widely used to modify the oxygen amount

Electronic supplementary material The online version of this article (<https://doi.org/10.1007/s10008-018-4037-5>) contains supplementary material, which is available to authorized users.

✉ D. A. L. Almeida
dalva.dri@gmail.com

¹ Instituto Nacional de Pesquisas Espaciais – INPE, Av. Dos Astronautas, 1758, São José dos Campos 12227-010, Brazil

and the oxygen functional groups on the carbon material surface [13–15]. According to Berenguer et al. [14], the chemical modification is widely used, but it is considered not suitable enough for controlling and modifying easily and selectively the surface chemistry of carbon materials. On the other hand, Desimoni et al. [15] showed that chemical oxidation by dilute potassium permanganate in concentrated sulfuric acid is reproducible by adjusting temperature, time of treatment, permanganate concentration, and the use of a conditioning (cleaning) treatment before the oxidation. The electrochemical modification has been considered a promising technique due to some advantages such as the reproducibility of the reaction conditions and selectivity and controllability of the oxidation and reduction processes [14, 16]. Currently, the literature has reported that the incorporation of heteroatoms like oxygen and nitrogen into carbon-based materials improves their specific capacitance because the heteroatoms are responsible for inducing pseudocapacitive behavior besides increase their polar properties [17].

The use of both oxidation treatments in CF with different HTT is not well understood, and there are no papers in the literature that show a relationship between the CF surface functionalities after oxidation treatments and their capacitive properties. It is known that different oxygen-containing groups are produced using various techniques or exposures. The result of the oxidation process as a function of both the amount of oxygen and the type of carbon-oxygen groups may also depend on the CF surface nature [4, 18].

In this work, two different chemical and electrochemical oxidation treatments were performed to activate CF surfaces produced at different heat treatment temperatures (HTT) of 1000, 1500, and 2000 °C. This variation is very important because as the HTT increase, the CF structural organization as well as its electrical conductivity also increases [19]. The samples without treatment (WT) and with chemical (CT) and electrochemical treatments (ET) were systematic analyzed by field emission gun-scanning electron microscopy (FEG-SEM), X-ray diffraction (XRD), Raman spectra, and X-ray photoelectron spectroscopy (XPS). The electrochemical characterizations were carried out by cyclic voltammetry (CV), charge/discharge curves, and electrochemical impedance spectroscopy (EIS) to analyze their performance as electrodes applied to supercapacitor devices.

Experimental

CF samples were produced from polyacrylonitrile (PAN) precursor at HTT of 1000, 1500, and 2000 °C and named as CF1000, CF1500, and CF2000, respectively. The temperature step was 330 °C/h under nitrogen atmosphere. The maximum temperature was kept for 30 min and then cooled down to room temperature. The CF samples were cut in 1 cm² size

and weighed. The sulfochromic solution (H₂SO₄/K₂Cr₂O₇) used in the chemical treatment (CT) was prepared dissolving 10 g K₂Cr₂O₇ into 50 mL of deionized water. Under constant stirring, 100 mL sulfuric acid (95%) was added slowly to keep the room temperature. This procedure was already used for Cheng et al. [20] for carbon paper activation. The CF samples were dispersed in boiling acetone for 5 min. Subsequently, they were washed with distilled water, immersed in H₂SO₄/K₂Cr₂O₇, and sonicated for 5 min. For electrochemical treatment (ET), the CF electrodes were anodically polarized using as electrolyte 0.5 mol L⁻¹ H₂SO₄ in a fixed potential of 2.0 V for 30 min adapted from the Wang et al. [2], using a conventional three-electrode cell with Ag/AgCl/KCl_(sat) and Pt mesh as reference and counter electrodes, respectively. Morphological, structural, and surface chemical changes were investigated by FEG-SEM from a TESCAN MIRA 3 microscope system; XRD patterns were carried out using a PANalytical model X'Pert Powder diffractometer with the Cu-Kα (λ = 1.54 Å), set at 45 kV and 25 mA, in the ω/2 θ configuration with ω = 1° and 2 θ varying from 10° to 80°; Raman spectra were recorded by a Horiba Scientific LabRAM HR Evolution microscope system with laser beam line of 514 nm; and XPS measurements were taken on a Kratos Axis Ultra XPS spectrometer using a monochromated Al-Kα (1486.5 eV) X-ray radiation at 15 kV and 150 W. The emitted photoelectrons were detected using a hemispherical analyzer of 15 μm spatial resolution. Broad scans were used for elemental quantification, and pass energy of 40 eV was used for high resolution scans on specific atomic peaks. The energy instrument resolution was 0.58 eV and estimated from the full width at half maximum of the XPS Ag 3d_{5/2} of a pure silver target. Spectroscopic data were processed in CasaXPS, version 2.3.16. The electrochemical characterization of the electrodes was studied by EIS measurements at open circuit potential (OCP) in 1 mol L⁻¹ H₂SO₄ with ± 10 mV of the potential amplitude in the frequency range of 10⁻³ to 10⁵ Hz, CV, and charge/discharge tests. All measurements were performed in 1.0 mol L⁻¹ H₂SO₄ solution.

Results and discussion

Morphological characterization

Figure 1 shows the surface morphologies of the CF heat treated at 1000, 1500, and 2000 °C and their respective chemically and electrochemically oxidized materials. The effect of heat treatment is difficult to visualize for both CF1000 and CF1500. On the other hand, the grooves and surface roughness of CF2000 (Fig. 1c) seem to increase. The fiber diameter was not determined due to the high variation in each sample and a slight variation after oxidation treatments that could lead to an incorrect average result. Also, in the HTT range studied,

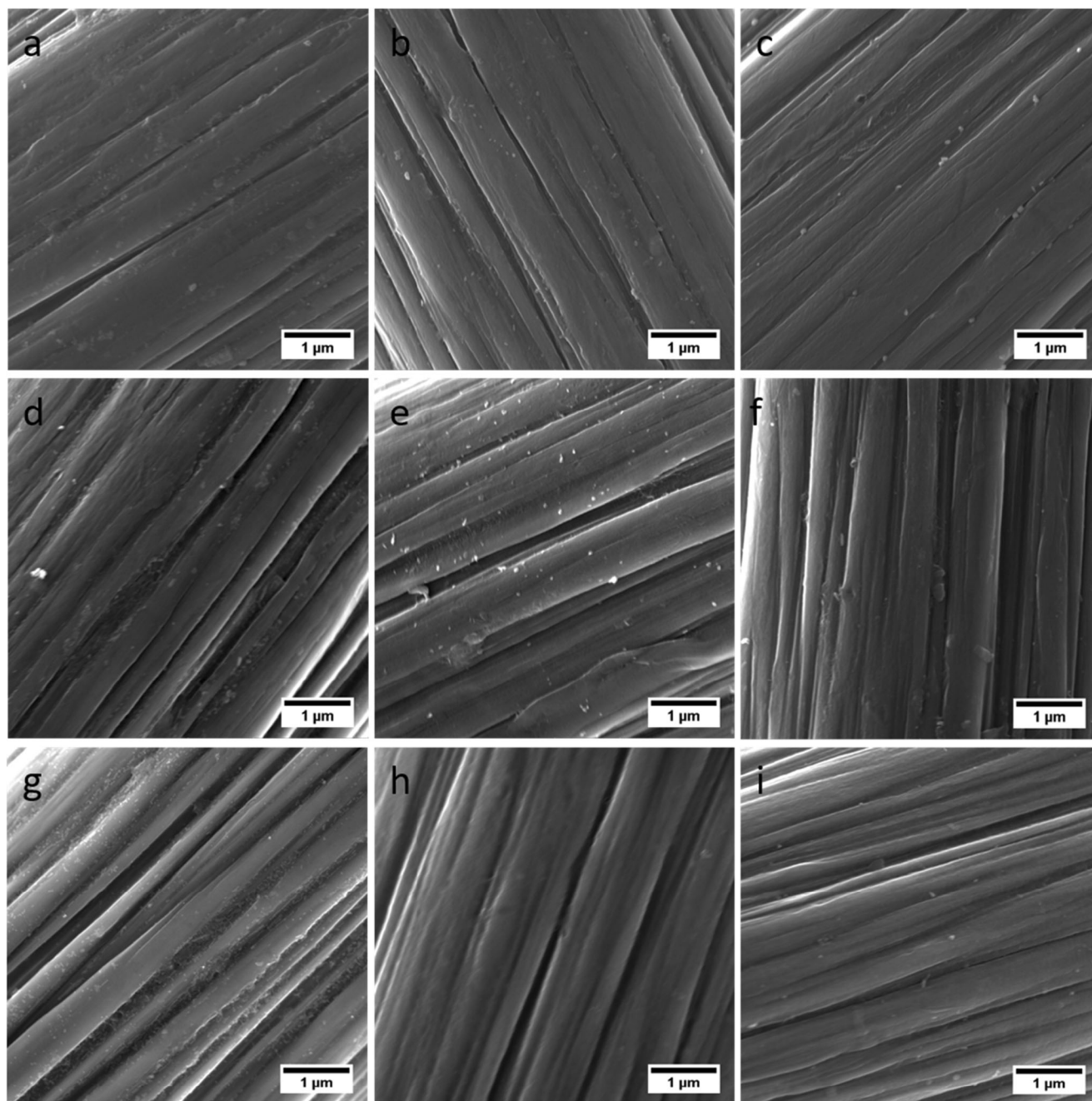


Fig. 1 FEG-SEM images of **a** CF1000WT, **b** CF1500WT, **c** CF2000WT, **d** CF1000CT, **e** CF1500CT, **f** CF2000CT, **g** CF1000ET, **h** CF1500ET, and **i** CF2000ET

there are two processes influencing the fiber diameter: (1) denitrogenation, which can bloat the fiber due to the high pressure created during the nitrogen gas evolution and leads to increased diameter; (2) graphitization, which leads to fiber shrinkage and increase densification [21]. According to Gao et al. [21], the average fiber diameter increases with increasing HTT until 1900 °C and decreases sharply after HTT above 1900 °C. After CT and ET, it can be clearly noted an increase in the grooves of the samples that probably increases their surface area (Fig. 1d–i). This behavior was more pronounced

for CF1000ET as seen in Fig. 1g. According to literature, the surface roughness of the treated fibers can increase due to the fact that oxidative treatment may promote controlled exfoliation of the first graphitic layers [22].

Surface and structural characterizations

Surface analyses after CT and ET of CF with different HTT were examined by XPS measurements. Table 1 shows the carbon, oxygen, and nitrogen atomic percentage obtained

Table 1 Atomic percentage of carbon, oxygen, and nitrogen of CF before and after chemical and electrochemical treatments

Sample	Composition (atomic %)		
	C1s	O1s	N1s
CF1000WT	82.79	12.81	4.40
CF1500WT	94.57	5.43	
CF2000WT	96.06	3.94	
CF1000CT	74.48	22.10	3.42
CF1500CT	86.92	13.08	
CF2000CT	93.13	6.87	
CF1000ET	68.05	27.80	4.15
CF1500ET	82.97	17.03	
CF2000ET	83.35	16.65	

from the survey scans. The presence of nitrogen is notice only on sample treated up to 1000 °C coming from the polyacrylonitrile precursor and is totally removed after 1500 °C HTT. An increase in the carbon content with HTT is expected, reaching a maximum value of 96.1% for CF2000 sample. The oxidation treatment does not change this trend of gradual increase in carbon content in samples with higher HTT. The introduction of oxygen to CF surface can be observed for both oxidation treatments in which electrochemical treatment is more severe, resulting in a higher percentage of oxygen than chemical treatment. Berenguer et al. [14] compared chemical and electrochemical treatments of activated carbon and also found that anodic treatment produced a higher oxidation degree than classical chemical oxidants like HNO₃, H₂O₂, and (NH₄)₂S₂O₈.

The graphitic carbon is the predominant C1s binding energy and increased with HTT, but it usually decreases with oxidation treatments [4, 16]. In this work, after CT, the percentage of atomic carbon decreased for CF1000, CF1500, and CF2000 samples, as expected. Similarly, for ET, the percentage of carbon loss was more pronounced for the three samples, indicating that this treatment was more severe. The literature reports that the capacitance improvements are probably dependent on the kind of oxygen functional groups present on

the electrode surface and not only on their amount [23]. According to Milczarek et al. [16], the C–OH and C=O functional groups increase the specific capacitance, while COOH group shows opposite behavior. In order to investigate the functional groups formed after oxidation treatments, C1s region was deconvoluted assuming the possible presence of six peaks assigned according to the literature [2, 24–26]: graphitic (~284.4 eV), β-carbon (~285.2 eV), hydroxide or ether (~286.1 eV), carbonyl (~287.7 eV), carboxyl or ester (~288.8 eV), and π–π* shake-up (~290.6 eV). The percentages of each functional group are shown in Table 2. The curve fitting for C1s region of CF without treatment and after chemical and electrochemical treatments are given in Online Resource 1.

For samples chemically modified, CF1000CT presents the largest increase for the carbonyl group varying from 7.0 (CF1000WT) to 18.1%. On the other hand, the electrochemical treatment increases the graphitic carbon for CF1000 probably due to removal of amorphous carbon. However, the largest presence of carboxylic group on CF1000ET demonstrates that this sample suffered higher oxidation, which can be related to its structural organization that is more susceptible to the action of severe oxidative treatment. In opposite way, CF2000 electrochemical treated exhibits the lowest value of carboxylic groups and the highest value of carbonyl group.

XRD patterns of CF samples heat treated at 1000, 1500, and 2000 °C without and after the respective chemical and electrochemical treatments are shown in Fig. 2. HTT effect increase is mainly observed in the narrowing and symmetry of (002) peak width. Additionally, the (004) peak appears after heat treatment at 1500 °C. Figure 3 shows the effects of chemical and electrochemical oxidations in CF with different HTT for the interlayer spacing (d_{002}), crystallite height (L_c), and crystallite width (L_a). The Bragg's law, $d_{002} = \lambda/2\sin\theta$ was used to calculate interlayer spacing, where λ is the radiation wavelength 0.154 nm and θ is the ($2\theta/2$) Bragg angle of (002) band (in rad). The Scherrer's equations, $L_c = 0.89\lambda/B\cos\theta$ and $L_a = 1.84\lambda/B\cos\theta$, were used to determine the crystallite height and crystallite width, respectively, where B is the full

Table 2 Percentages of each surface functional group from C1s spectra of carbon fiber

Sample	C–C	β-carbon	C–O or C–OH	C=O	COOH	π → π*
CF1000WT	50.88	11.10	25.41	7.00	3.72	1.88
CF1500WT	61.62	12.51	17.60	1.66	4.66	1.95
CF2000WT	72.20	1.81	15.97	6.12	0.54	3.36
CF1000CT	46.22	11.15	18.08	18.09	5.67	0.78
CF1500CT	62.98	8.19	14.23	10.24	0.56	3.81
CF2000CT	58.75	16.71	13.62	6.47	1.72	2.73
CF1000ET	62.96	6.21	15.73	7.88	7.16	0.07
CF1500ET	65.26	0.14	14.63	13.77	4.89	1.30
CF2000ET	61.20	12.77	7.79	14.76	0.92	2.55

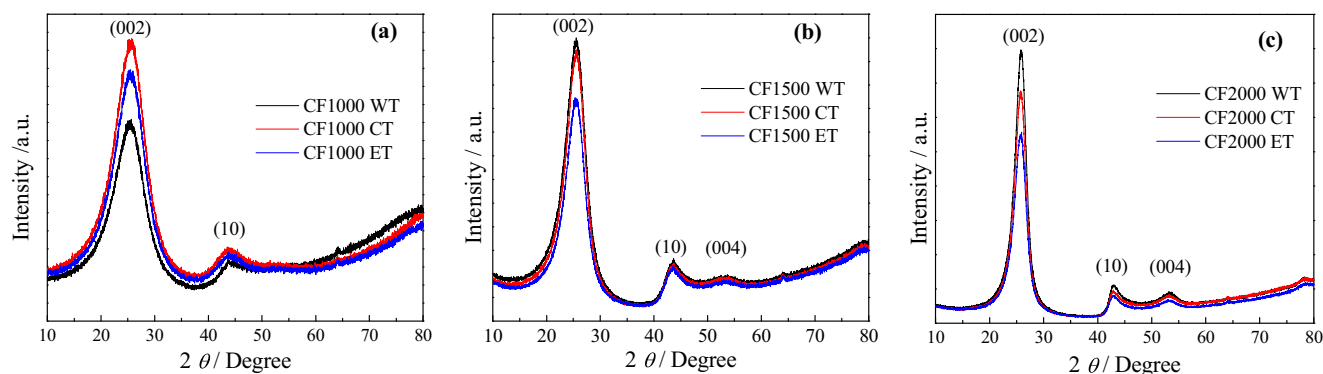


Fig. 2 X-ray diffraction patterns of **a** CF1000WT, **b** CF1500WT, and **c** CF2000WT and their respective chemical and electrochemical oxidized samples

width at half maximum and θ is the $(2\theta/2)$ Bragg angle (in rad) of (002) band for L_c or (100) band for L_a [26, 27]. HTT effect is evident in the improvement of graphitic order by d_{002} decrease followed by L_c and L_a increase for CF1000, CF1500, and CF2000, respectively. Lower values of d_{002} indicate less defects on graphitic layers leading, consequently, to a better packing [28]. Comparing d_{002} values of CF1000, the CT and ET seems to improve the graphitic layers packing in comparison to that for this sample without treatment. The introduction of oxygen by both treatments, as revealed by XPS, creates active centers that may help to suppress the increase of the

interlayer spacing by forming strong chemical bonds between carbon and oxygen atoms [29, 30]. For CF1500, both oxidation treatments do not affect the d_{002} , while for CF2000, there is a small increase in d_{002} . As the CF2000 microstructure is more organized, the oxidation treatments only generate defects, increasing it interlayer spacing.

L_c represents the stacking height of graphitic layers [26], and it is shown as a function of HTT for both oxidation treatments in Fig. 3b. When the CT and ET effects are analyzed for CF1000, the crystallite height is preserved in relation to that for this fiber without treatment. For CF1500, L_c value slightly

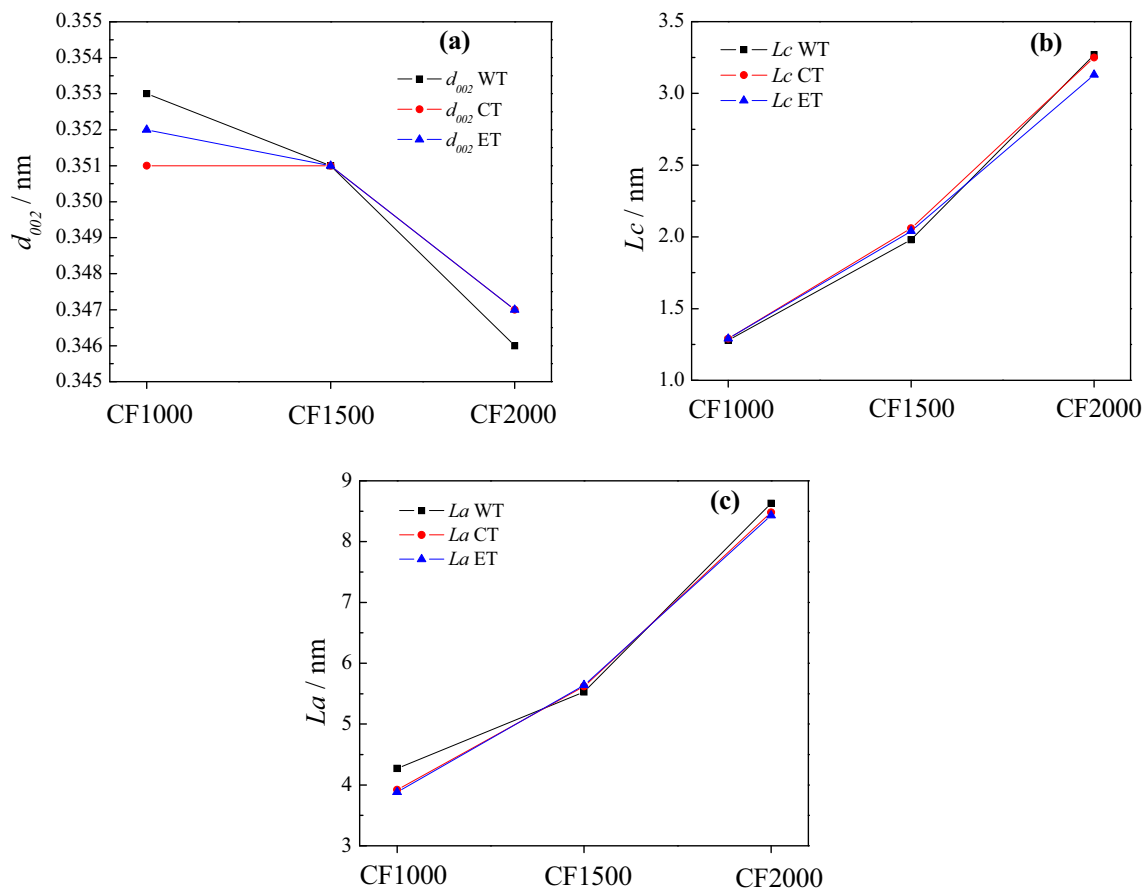


Fig. 3 **a** Interlayer spacing (d_{002}), **b** crystallite height (L_c), and **c** crystallite width (L_a)

increases after both oxidation treatments, while for CF2000, there is a decrease mainly for ET. This behavior may be attributed to surface oxygen contents on this ET fiber that increased four times according to Table 1. Collins et al. [26] have discussed this tendency on oxidized activated carbon and explained that since the edges of stacked graphene sheets become excessively concentrated with surface oxygen groups, more energy is necessary to keep the stacked formation of graphene sheets. Consequently, the average crystallite height decreases as a function of the defect sites increases. This effect is also confirmed by d_{002} results (Fig. 3a) which shows an increase in interlayer spacing for both CT and ET CF2000, which can be associated to the steric hindrance.

Taking into account the La values (Fig. 3c), a larger variation is noticed for CF1000 after both treatments. This performance can be related to its lowest structural ordering, which enables higher modification after oxidation treatments at the in-plane extent. CF1500 presented slightly variation between the two different treatments, tending to an improvement. On the other hand, CF2000 showed an opposite effect with both oxidation treatments, i.e., the crystalline width decreased slightly compared to untreated carbon fiber. Considering that XRD technique gives information of the material bulk, this behavior may be associated to more contribution of the CF2000 bulk where it is not affected by oxidative treatment, as can be seen in the FEG-SEM images. In the opposite way, the oxidative treatment achieved deeper layers of CF1000, due to the fact that crystallite of graphite was less organized and more susceptible to oxidative treatments, resulting to more pronounced decrement of La values. Furthermore, because different mechanisms and factors may be acting for the in-plane growth and the growth normal to the plane, La values do not necessarily have a parallel trend with Lc [31].

Raman analyses give the information of the carbon surface with a sampling depth of about 100 nm [32]. Thereby, it can detect changes in structural order after surface treatments, unlike XRD technique, which gives information of the core part that is not so affected by the oxidative treatment. Figure 4 shows the normalized first-order Raman spectra of each CF sample set (CF1000, CF1500, and CF2000) with their

respective chemical and electrochemical treatments. An increase of graphitization index results in a decrease of D and G band widths, located around 1350 and 1590 cm^{-1} , respectively. The intensity ratio of D to G bands (I_D/I_G) is a parameter to quantify the degree of disorder in carbon material, where lower I_D/I_G indicates a lower disorder in carbon material samples [33]. Figure 5 shows the I_D/I_G ratio of CF samples as a function of HTT for the three conditions: WT, after CT, and after ET. Analyzing CF1000 and CF1500 samples, the graphitic ordering increased as I_D/I_G ratio decreased after both treatments. For CF2000, the oxidative treatments have an opposite effect, increasing its structural disorder. Generally, oxidation treatments may introduce some degree of disorder at the surface level [34]. In this sense, I_D/I_G ratio for CF1000 and CF1500 oxidized samples is quite questionable. According to Samuel et al. [35], I_D/I_G ratio is not a complete criterion and must be used along with complementary techniques. This is because samples with low HTT still present broad D and G bands hindering a reliable quantification. That is why changes in Raman spectra after oxidation on CF1000 and CF1500 samples are very small and for CF2000 are more visible. As reported by Samuel et al. [35] and Gonçalves et al. [36], I_D/I_G ratio increases after heat treatment at various temperatures and decreases only at 2000 °C. However, CF1500 oxidized samples follow the same tendency as observed from XRD analyses, i.e., a slightly graphitic ordering improvement after both oxidation treatments. Similarly, CF2000 Raman results are in good agreement with XRD, in which ET generates higher disorder than that for CT. The electrochemical treatment seems to be more severe for CF2000 sample surface since a significant change can be observed for its Raman spectrum in Fig. 4c, such as the following: the increase in D band intensity that is related to the increase of unaligned regions [37]; the increase in the full width at half maximum of D and G band associated with an increase in disorder and in the oxygen percentage of CF surface [38, 39]; the increase in the band at 1500 cm^{-1} (also called D3 or D'') related to amorphous carbon entities, like organic molecules, stacking faults, and non-graphitic carbon with a high density of oxygen functional groups as can be verified by XPS analysis [40, 41]; and the

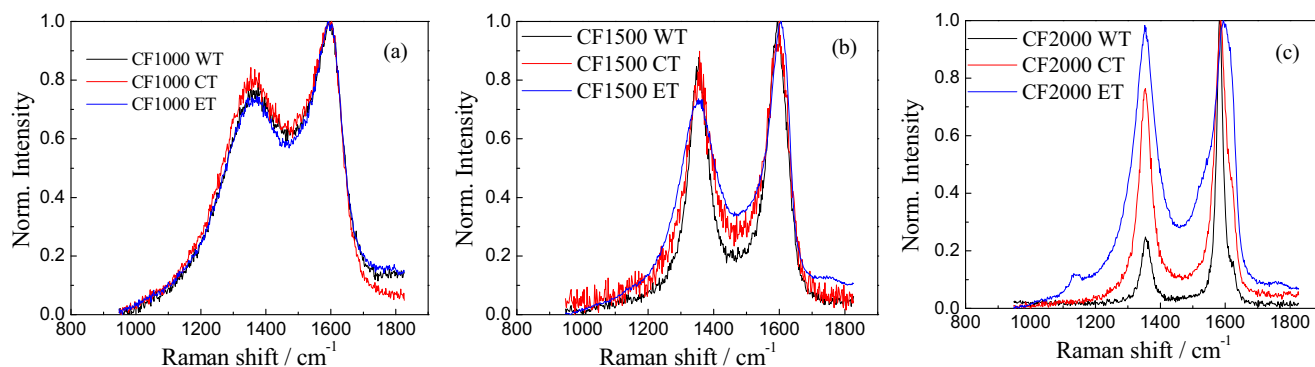


Fig. 4 Raman spectra of **a** CF1000WT, **b** CF1500WT, and **c** CF2000WT and their respective chemical and electrochemical oxidized samples

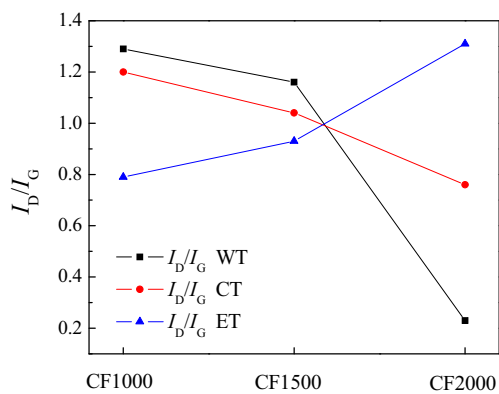


Fig. 5 I_D/I_G ratio of CF heat treated at various temperatures and with different oxidation treatments

appearance of D4 or I band at around 1140 cm^{-1} related to transpolyacetylene or ionic impurities [40, 42].

Electrochemical measurement

The CV curves of all electrodes were obtained from -0.1 to 0.8 V and at scan rate of 25 mV s^{-1} , using 1.0 mol L^{-1} of H_2SO_4 as electrolyte. Figure 6a–c shows the CV curves for CF1000, CF1500, and CF2000 without and after the two oxidation processes. By comparing the three untreated fibers, it was observed that CF1000 has a capacitive current in the order of 10^{-3} A , whereas for both CF1500 and CF2000, these values are in the order of 10^{-5} A , which means that CF1000 presents a capacitive response two orders of magnitude larger than those for CF1500 and CF2000. In addition, for the more conductive CF electrodes (1500 and 2000), the cathodic currents start at lower potential as expected due to the increase in the carbon content with HTT, according to XPS analyses. After chemical treatment (CT), only CF1000 exhibited a capacitive profile as shown by the almost rectangular voltammogram with high current density, typical of the capacitor response. This results indicated that the CT was less severe for the CF1000 and favored the incorporation of carbonyl groups on its surface ($\text{C}=\text{O}$) without significant change in the first graphitic layers [43]. According to Yun et al. [17], the

presence of these functional groups on the electrode surface improves the supercapacitor performance due to increase its hydrophilic polar sites enhancing its wettability favoring Faradic reactions. On the other hand, the CF1500 and CF2000 did not show the same behavior with CT. These fibers were extremely organized, and with few heteroatoms, consequently, the CT was less efficient to break the C–C bonds to give rise to edge carbon atoms allowing to incorporate a greater amount of heteroatoms as well as to create mesopores that enabled a more electrochemically active surface [14].

Otherwise, the ET provided better capacitive performances for the CF1500 and CF2000 because it promoted the incorporation of higher percentage of carbonyl groups on these CF surfaces than those for chemical treatment. According to Nian and Teng [23], after electrochemical treatment, the double-layer formation process occurs due to the presence of carbonyl or quinone-type site in the surface of the carbon that contributes for proton adsorption enhancing the capacitance. Besides, Faradaic reactions were also observed in the region between 0.4 and 0.45 V related to couple redox peaks for the CF1500 and CF2000 electrodes. These redox peaks may be explained by the presence of the quinone–hydroquinone or pyrone-like structures with pair redox, which present oxidation/reduction processes due to the oxygenated surface functionalities [16, 19], such as $\text{C}=\text{O}$ and $\text{C}-\text{O}$ obtained by the XPS data, showed in Table 2. For CF1000 after ET, it was observed a small distortion in the voltammogram for the current response, which may be attributed to electrolyte and electrode resistances. This result indicated that the ET is more severe for CF1000 because it not only removed the amorphous carbon and edge carbon atoms, but also created grooves as previously discussed in FEG-SEM images, which can originate micropore creation that may turn difficult the electrode wettability [44], resulting in more resistive behavior [17]. In addition it was observed an increase of functional groups COOH , responsible for the decrease of the capacitive effect [16]. Nonetheless, this effect was less evident with CT in CF1000 resulting in its lowest resistivity. These data corroborate with Raman analyses for CT treatment, where I_D/I_G decreases moderately for CF1000 and CF1500, except for CF2000. For ET treatment, the I_D/I_G

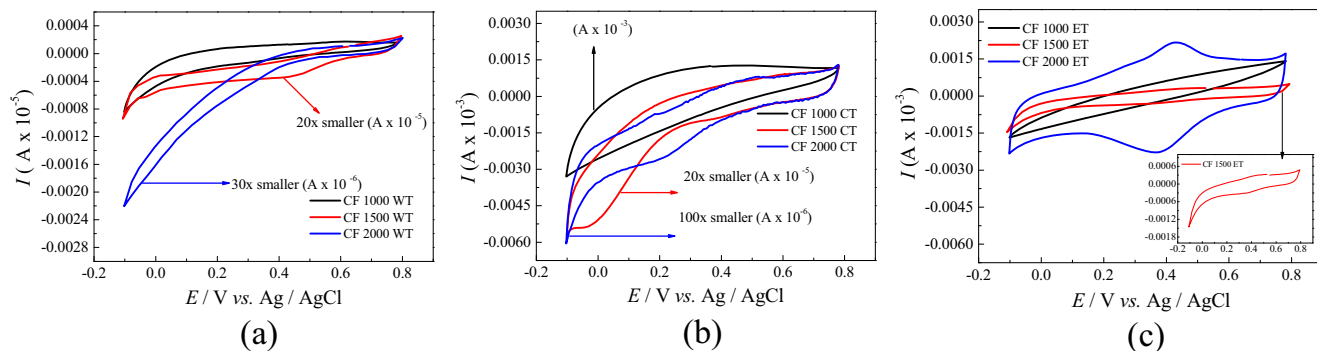


Fig. 6 Cyclic voltammetry of treated and untreated CF samples at 25 mV s^{-1} **a** CFs WT, **b** CFs CT, and **c** CFs ET

decreased dramatically for CF1000 and CF1500 and increased for CF2000. According to literature, the I_D/I_G ratio is used as an index to evaluate the level of destruction of the carbon surface structures that were subjected to an anodic oxidation. This modification in the surface structure gives rise to large numbers of edge carbon atoms that facilitate the bond with oxygenated functional groups [34].

Figure 7a–c illustrates the charge/discharge curves for CF1000, CF1500, and CF2000 electrodes without and after the two oxidation processes at 0.2 A g^{-1} current density. After CT, only CF1000 exhibited a long charge/discharge time, while for CF1500 and CF2000, these times did not change in relation to these samples WT. For ET, the CF1000 electrodes exhibited a non-linear charge/discharge whereas for CF1500 and CF2000 electrodes, the curve profiles are typical of the conventional symmetric capacitor. This behavior can be correlated with the presence of oxygen contents as well as the presence of C–OH and C=O oxygen functional groups obtained from the XPS analysis. These results corroborated with that reported by Chen et al., which demonstrated that these oxygen functional groups enhance the pseudocapacitive reactions [44]. In addition, all CF samples WT showed high value of the IR drop, where R is ohmic drop or resistance uncompensated. According to literature, the IR drop is a result of the association of resistance, which includes electrode and electrolyte resistances and denominated equivalent series resistance (ESR) [45]. For CF1500 and CF2000, it was not possible to measure IR values due to very low-charge storage. After the CT, IR drop of the CF1000 decreased of 0.5 for 0.2 V whereas for CF1500 and CF2000, no significant change occurred. On the other hand, for ET, the CF1500 and CF2000 electrodes showed IR drop values lower than that of CF1000, i.e., 0.04 and 0.07 V, for CF1500 and CF2000, respectively, while for CF1000, the IR drop value was 0.32 V. The smaller IR drop values may be related to the high conductivity of the electrodes. Thus, the electrochemical oxidation was more efficient for CF1500 and CF2000 electrodes, while the chemical oxidation improved the electrochemical performance of CF1000 electrode.

Cell capacitance values were determined by charge-discharge test from discharge curves at constant current according to the Eq. (1):

$$C_{sp} = I / [(dV/dt) \times m] \quad (1)$$

where I is constant current discharge curves, dV/dt is calculated from the slope of the discharge curve, and m is the mass of electrodes [46].

The specific capacitance values were calculated based on the weight of active materials for CF1000, CF1500, and CF2000 before and after the two oxidation processes in order to evaluate their capacitive performances. Figure 8a shows the specific capacitance as a function of the cycle numbers for all electrodes studied, obtained from Eq. (1). The initial capacitance values are around 20, 0.48, and 0.15 F g^{-1} , for the CF1000, CF1500, and CF2000 without treatment, respectively. After ET, the specific capacitance values of these electrodes increased significantly for 100, 111, and 72 F g^{-1} , for the three samples, respectively. After CT, only the CF1000 electrode presented a significant capacitance value increase, around 138 F g^{-1} while the CF1500 and CF2000 electrodes presented values of the 1.24 and 0.66 F g^{-1} . According to Stoller and Ruoff [46], electrodes with pseudocapacitive behavior can present large deviations in linearity resulting in the no longer symmetrical discharge curves. Thus, in this case, the use of slope dV/dt can lead to significant errors in the C_{sp} values. Taking into account, we also presented the calculations considering this methodology to compare C_{sp} values. Figure 8b showed the C_{sp} regarding method by Stoller and Ruoff [46], using two data points from the discharge curve, where $dV/dt = (V_{\max} - \frac{1}{2}V_{\max}) / (t_2 - t_1)$. This methodology was used just for the electrodes CF1000TC, CF1000ET, CF1500ET, and CF2000ET. For other electrodes, it was not possibly calculated due to extremely low values of time discharge and high values of IR drop, making it difficult to select the correct range of time and potential from the discharge curve. It was verified an increase in the capacitance values, i.e., at around 126, 130, and 80 F g^{-1} for CF1000ET, CF1500ET, and CF2000ET, respectively, and for CF1000CT at around 200 F g^{-1} .

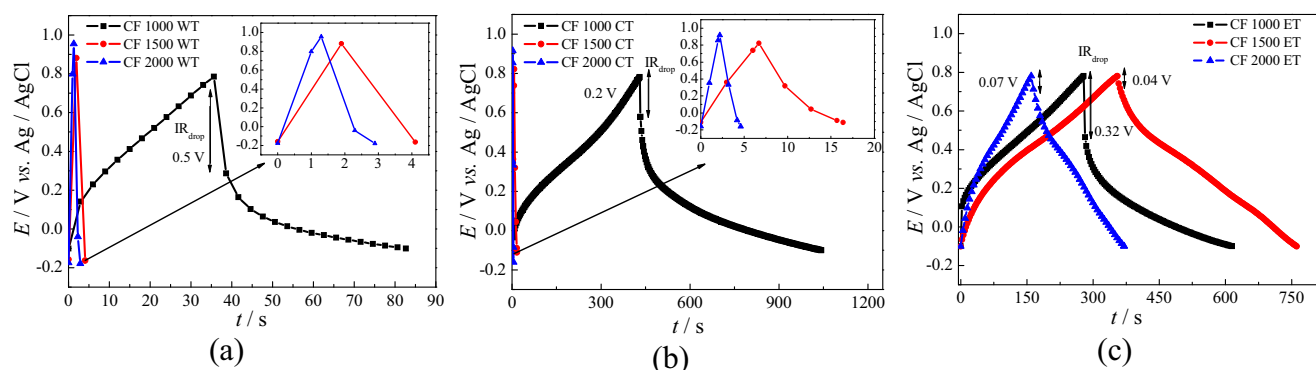


Fig. 7 Charge/discharge curves of treated and untreated CF samples at $j = 0.2 \text{ A g}^{-1}$ **a** CFs WT, **b** CFs CT, and **c** CFs ET

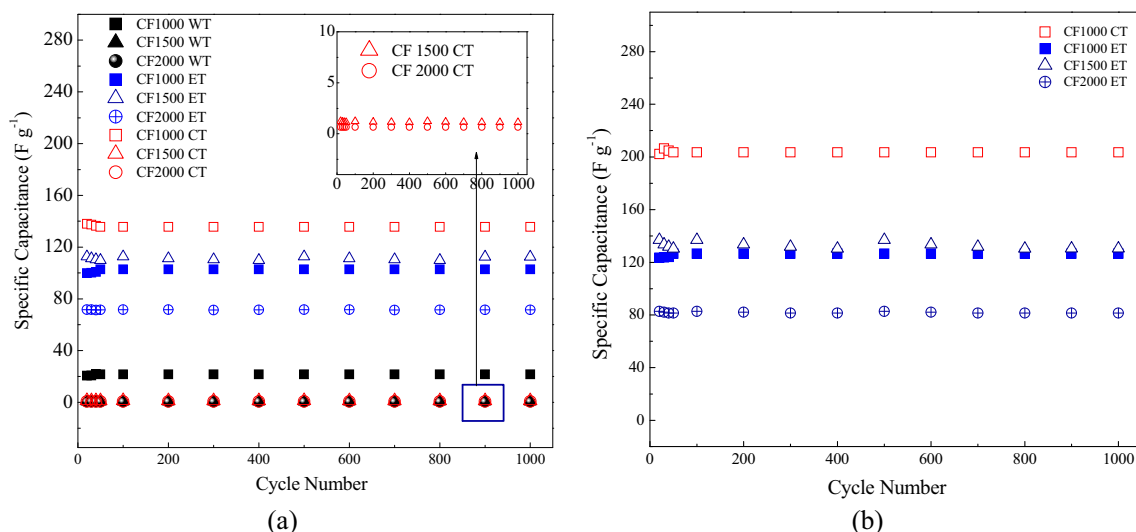


Fig. 8 Specific capacitance of CF1000, CF1500, and CF2000 without treatment and after the two treatments: electrochemical (ET) and chemical (CT) at $j \pm 0.2 \text{ A g}^{-1}$ **a** considering the total slope dV/dt and **b** $dV/dt = (V_{\text{max}} - 1/2V_{\text{max}})/(t_2 - t_1)$

Therefore, the ET was more efficient for CF1500 and CF2000, while CT was best for CF1000. This behavior can be attributed to the surface area increase due to the suitable grooves and roughness appearance in CF surface as shown by FEG-SEM images in Fig. 1d, h, i. Another important contribution may be related to the incorporation of oxygen atoms by the oxidative process that promoted the hydrophilic character on the CF surfaces. According to the literature, the incorporation of heteroatoms like oxygen and nitrogen into carbon-based materials improves their specific capacitance because the heteroatoms are responsible for inducing pseudocapacitive behavior [17]. These results corroborate with the XPS and Raman results, which showed oxygen atoms as well as the structural disorder increase, respectively.

In addition, the coulombic efficiencies were calculated using Eq. (2):

$$\eta = (t_c/t_d) \times 100\% \tag{2}$$

where t_c is the time charge and t_d is the time discharge [47]. Table 3 showed the coulombic efficiency values for all

Sample	η (%)
CF1000WT	75
CF1500WT	86
CF2000WT	43
CF1000CT	72
CF1500CT	95
CF2000CT	63
CF1000ET	82
CF1500ET	87
CF2000ET	78

electrodes. Comparing η values of the samples before and after the two oxidation processes, it was verified that ET increased the coulombic efficiency for CF1000 and CF2000 whereas CT enhanced for the CF1500 and CF2000. According to literature, decreasing η values as a function of cycling number is due to the non-reversible reactions within the cell [46]. Although η values of our electrodes did not achieved 100%, it is noteworthy that the coulombic efficiency for all samples kept a constant value during cycling number (see Online Resource 1), indicating good electrochemical reversibility.

Table 4 shows some results of specific capacitance published in the literature for carbon fibers with different oxidative treatments. The results of specific capacitance with approximate conditions used in this work such as HTT, current density, and electrolyte were selected. It is important to point out that this study presents a one-step process for both oxidative treatments. By comparison, according to Table 4, we showed significant capacitance increase with simple and effective methodologies.

The Nyquist diagrams for CF1000 electrodes without and after the two oxidation processes are presented in Fig. 9a–b. It is important to point out that the vertical line in the diagrams, almost parallel to $-Z''$ -axis represents an equivalent circuit consisting of a resistance in parallel with a capacitor. For CF1000 electrodes, the capacitive behavior was observed in low-frequency region after both treatments [17]. Figure 9a inset shows a zoom view for medium-frequency region while for high-frequency region, it is better visualized in Fig. 9b. Electrochemical parameter qualitative values of the CF1000 electrodes can be obtained analyzing the Nyquist diagrams. For CF1000 samples WT and after CT, warped semi-cycles in the high-frequency region were observed, in which the first value extrapolated with the real Z' -axis is attributed to the

Table 4 Overview of some results published in the literature for specific capacitance of carbon fibers with various oxidative treatments

Carbon electrode	HTT	Oxidative treatment	Electrolyte	Electrochemical cell	Cs (F/g)	Ref.
PAN-based nanofibers paper	1000 °C	Activation at 1000 °C under CO ₂ atmosphere	1 M H ₂ SO ₄	Three electrodes	~ 170	[48]
PAN-based activated carbon fibers	900 °C	Nitric acid	1 M H ₂ SO ₄	Two electrodes	~ 120	[49]
Activated carbon fiber cloth	*N.A.	Electrochemical oxidation	0.5 M H ₂ SO ₄	Two electrodes	170	[50]
Activated carbon fibers papers	900 °C	Activation under O ₂ at 325 °C	1 M H ₂ SO ₄	Three electrodes	157	[51]
Coal-based pitch fibers	240 °C	Chemically activated after impregnation with NaOH at 900 °C	1 M H ₂ SO ₄	Two electrodes	109	[52]
Activated carbon fiber cloth	*N.A.	Electrochemical activation	3.75 M H ₂ SO ₄	Two electrodes	169	[16]
PAN-based activated carbon fabric	N.A.	Thermal treatment at 250 °C under O ₂ atmosphere	1 M H ₂ SO ₄	Two electrodes	150	[53]

*N.A. not available

solution resistance, at around 1 Ω , using OCP. Also, the transfer charge resistance (R_{ct}) is observed at second intersection of semi-cycle with Z' -axis [54]. The CF1000WT showed R_{ct} at around 4 Ω . After CT, this value remained unchanged while after its electrochemical oxidation, the R_{ct} value was 400 Ω . The chemically treated CF1000 sample showed a more capacitive profile which may be ascribed to the moderate increase of oxygen amount on its surface [44], verifying in its XPS analysis. However, the electrochemical oxidation can promote the excessive incorporation of oxygen groups and exfoliation of the first graphitic layers with edge carbon atoms resulting in a reorganization of the surface layers, which would also explain the I_D/I_G ratio decrease from 1.3 to 0.8 as shown in Raman analysis. Furthermore, Fig. 1g showed the excessive increase of grooves and surface roughness in CF1000 after ET. These results confirmed the resistive voltammetric behavior of this sample.

The Nyquist diagrams for CF1500 before and after the two treatments are presented in Fig. 9c–d for all frequency ranges studied. The Nyquist diagrams showed the capacitive behavior in the high-frequency region very similar to those observed in the CF1000 results (Fig. 9b). The R_{ct} for CF1500WT was around 0.6 Ω . With chemical oxidation, this value remained unchanged while after the electrochemical oxidation, the R_{ct} value was 50 Ω . Nevertheless, observing the expanded Nyquist diagrams in the medium-frequency ranges (inset Fig. 9a, c), the diameter of the semi-cycle for the CF1500ET was smaller than that for the CF1000ET. This result was much lower when compared with that obtained for CF1000, indicating high electronic transference velocity of this electrode due to its higher surface area available for the electrolyte [55]. In addition, the ET may incorporate more oxygen atoms in CF1500 structure, promoting a surface wettability; as a consequence, the electron transfer occurs more easily [44], which explains its higher charge/discharge times were observed in galvanostatic tests.

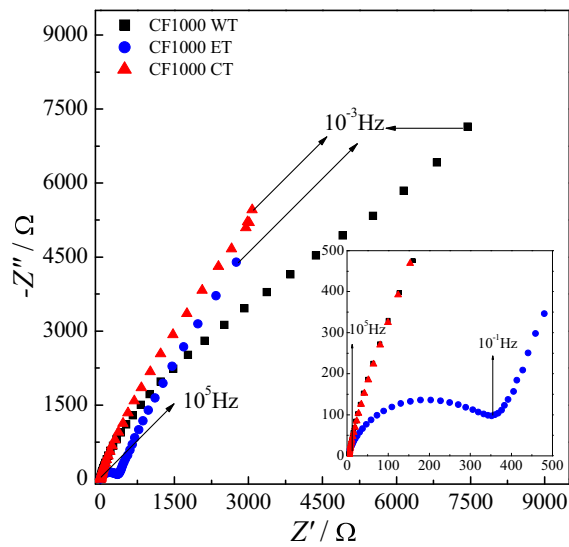
The Nyquist diagrams for CF2000 before and after the two treatments are presented in Fig. 9e–f for all frequency ranges

studied. The results are comparable to those for CF1500. This similar behavior was attributed to the fact that both materials were obtained from high HTT, close to graphitization process. The CF2000WT electrode presented R_{ct} value at around 0.6 Ω . With chemical oxidation, this value did not change while that after electrochemical oxidation, the R_{ct} value was estimated at around 1.8 Ω , which represents the smallest R_{ct} value. This result is 200 times smaller than that for CF1000ET and 25 times smaller than that for CF1500ET. The CF2000ET presented the highest structural organization promoting the lowest electrochemical oxidation effect on its surface. It is noteworthy that the electrochemical oxidation was less aggressive for CF2000 surface; as consequence, a capacitance value increase was observed only in this electrode. This increase was attributed to its high percentage C–OH and C=O groups not to mention its surface wettability increase [56]. It is clearly that the oxidative processes were important to the active surface of CF samples when applied as an electrode for supercapacitor.

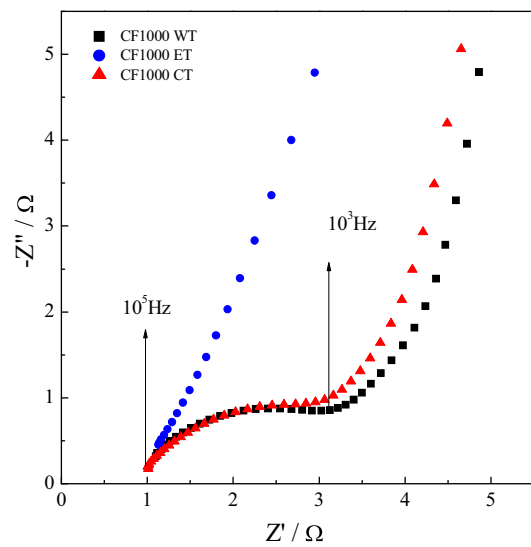
Conclusion

Carbon fiber samples obtained from different HTT and activated through oxidative processes were suitable for application as electrode materials in supercapacitors. After chemical and electrochemical oxidative processes on the CF samples, it was observed an increase in their roughness surface, which probably increased their surface area. In addition, XRD results revealed slightly variations between different oxidation treatments for each HTT, indicating that they slightly affected the core of CF samples. A capacitive behavior was observed for CF1500 and CF2000 after electrochemical oxidation in CV

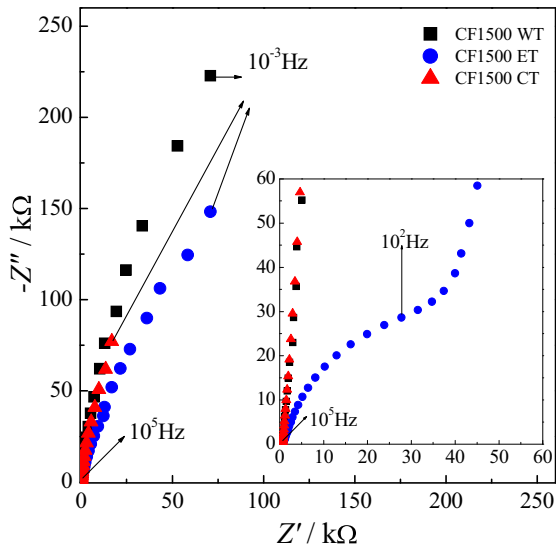
Fig. 9 Nyquist plots for **a** CF1000, **c** CF1500, and **e** CF2000 in the whole range and zoom medium frequency; inset: medium-frequency region; and **b**, **d**, **f** zoom of high-frequency interval for electrodes before and after the two treatments



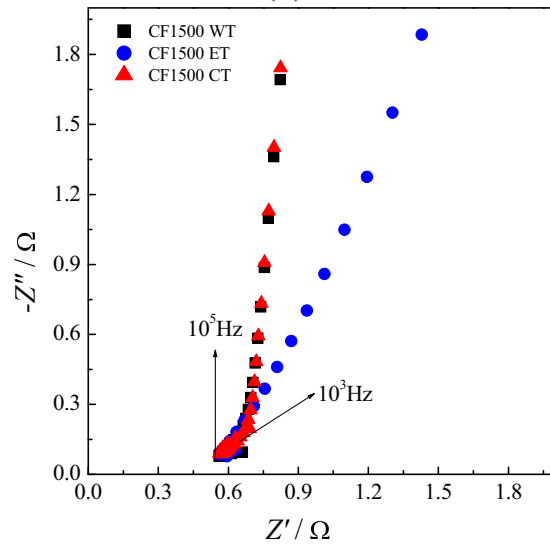
(a)



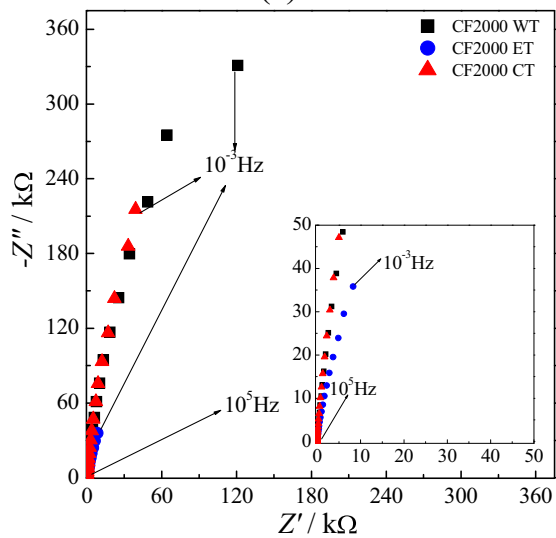
(b)



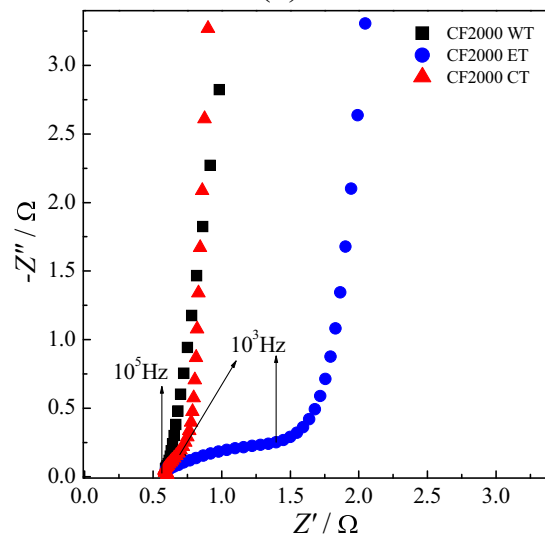
(c)



(d)



(e)



(f)

measurements due to the incorporation of the higher percentage C–OH and C=O groups on these surfaces. However, the EIS analyses showed that the chemically treated CF presented lower R_{ct} values when compared to electrochemically treated CF. Particularly, CF1000 chemically treated exhibited the best performance considering both charge/discharge curves and EIS measurements. This behavior can be attributed to the presence of oxygen atoms on its surface, which favored pseudocapacitive reactions. In general, the two oxidation processes contributed to the increase of the specific capacitance values for all samples studied. CT was more suitable for samples with lower HTT whereas ET was more efficient for samples obtained to a high HTT.

References

- Staiti P, Lufano F (2010) Investigation of polymer electrolyte hybrid supercapacitor based on manganese oxide-carbon electrodes. *Electrochim Acta* 55(25):7436–7442
- Wang Y-Q, Viswanathan H, Audi AA, Sherwood PMA (2000) X-ray photoelectron spectroscopic studies of carbon fiber surfaces. 22. Comparison between surface treatment of untreated and previously surface-treated fibers. *Chem Mater* 12(4):1100–1107
- Tong Y, Wang X, Su H, Xu L (2011) Oxidation kinetics of polyacrylonitrile-based carbon fibers in air and the effect on their tensile properties. *Corros Sci* 53(8):2484–2488
- Yue ZR, Jiang W, Wang L, Gardner SD, Pittman CU Jr (1999) Surface characterization of electrochemically oxidized carbon fibers. *Carbon* 37(11):1785–1796
- Kim BH, Yang KS (2013) Enhanced electrical capacitance of porous carbon nanofibers derived from polyacrylonitrile and boron trioxide. *Electrochim Acta* 88:597–603
- Chung DDL (2004) Electrical applications of carbon materials. *J Mater Sci* 39(8):2645–2661
- Inagaki M, Konno H, Tanaiki O (2010) Carbon materials for electrochemical capacitors. *J Power Sources* 195(24):7880–7903
- Kim C, Choi YO, Lee WJ, Yang KS (2004) Supercapacitor performances of activated carbon fiber webs prepared by electrospinning of PMDA-ODA poly(amic acid) solutions. *Electrochim Acta* 50(2-3):883–887
- Xia K, Gao Q, Jiang J, Hu J (2008) Hierarchical porous carbons with controlled micropores and mesopores for supercapacitor electrode materials. *Carbon* 46(13):1718–1726
- Chen YC, Hsu YK, Lin YG, Lin YK, Horng YY, Chen LC, Chen KH (2011) Highly flexible supercapacitors with manganese oxide nanosheet/carbon cloth electrode. *Electrochim Acta* 56(20):7124–7130
- Rahaman MSA, Ismail AF, Mustafa A (2007) A review of heat treatment on polyacrylonitrile fiber. *Polym Degrad Stab* 92(8):1421–1432
- Dai Z, Zhang B, Shi F, Li M, Zhang Z, Gu Y (2011) Effect of heat treatment on carbon fiber surface properties and fibers/epoxy interfacial adhesion. *Appl Surf Sci* 257(20):8457–8461
- Berenguer R, Marco-Lozar JP, Quijada C, Cazorla-Amorós D, Morallón E (2009) Effect of electrochemical treatments on the surface chemistry of activated carbon. *Carbon* 47(4):1018–1027
- Berenguer R, Marco-Lozar JP, Quijada C, Cazorla-Amorós D, Morallón E (2012) A comparison between oxidation of activated carbon by electrochemical and chemical treatments. *Carbon* 50(3):1123–1134
- Desimoni E, Salvi AM, Casella IG, Damiano D (1993) Controlled chemical oxidation of carbon fibres: an XPS-XAES-SEM study. *Surf Interface Anal* 20(11):909–918
- Milczarek G, Ciszewski A, Stepniak I (2011) Oxygen-doped activated carbon fiber cloth as electrode material for electrochemical capacitor. *J Power Sources* 196(18):7882–7885
- Yun YS, Lee ME, Joo MJ, Jin HJ (2014) High-performance supercapacitors based on freestanding carbon-based composite paper electrodes. *J Power Sources* 246:540–547
- Zhong C, Gong S, Jin L, Li P, Cao Q (2015) Preparation of nitrogen-doped pitch-based carbon materials for supercapacitors. *Mater Lett* 156:1–6
- Medeiros LI, Couto AB, Matsushima JT, Baldan MR, Ferreira NG (2012) Nanocrystalline diamond coating on carbon fibers produced at different temperatures: morphological, structural and electrochemical study. *Thin Solid Films* 520(16):5277–5283
- Cheng Z, Liu P, Guo B, Qiu Y, Xu P, Fan H (2015) Surface activation of carbon paper with potassium dichromate lotion and application as a supercapacitor. *Appl Surf Sci* 349:833–838
- Gao A, Su C, Luo S, Tong Y, Xu L (2011) Densification mechanism of polyacrylonitrile-based carbon fiber during heat treatment. *J Phys Chem Solids* 72(10):1159–1164
- Kainourgiou P, Kartsonakis IA, Dragatogiannis DA, Koumoulos EP, Goulis P, Charitidis CA (2017) Electrochemical surface functionalization of carbon fibers for chemical affinity improvement with epoxy resins. *Appl Surf Sci* 416:593–604
- Nian YR, Teng H (2003) Influence of surface oxides on the impedance behavior of carbon-based electrochemical capacitors. *J Electroanal Chem* 540:119–127
- Desimoni E, Casella GI, Morone A, Salvi AM (1990) XPS determination of oxygen-containing functional groups on carbon-fiber surfaces and the cleaning of these surfaces. *Surf Interface Anal* 15(10):627–634
- Weitzsacker CL, Xie M, Drzal LT (1997) Using XPS to investigate fiber/matrix chemical interactions in carbon-fiber-reinforced composites. *Surf Interface Anal* 25(2):53–63
- Collins J, Zheng D, Ngo T, Qu D, Foster M (2014) Partial graphitization of activated carbon by surface acidification. *Carbon* 79:500–517
- Musiol P, Szatkowski P, Gubernat M, Weselucha-Birczynska A, Blazewicz S (2016) Comparative study of the structure and microstructure of PAN-based nano- and micro-carbon fibers. *Ceram Int* 42(10):11603–11610
- Takai K, Oga M, Sato H, Enoki T, Ohki Y, Taomoto A, Suenaga K, Iijima S (2003) Structure and electronic properties of a nongraphitic disordered carbon system and its heat-treatment effects. *Phys Rev B* 67:1–11
- Nakamizo M, Tamai K (1984) Raman spectra of the oxidized and polished surfaces of carbon. *Carbon* 22(2):197–198
- Ong TS, Yang H (2000) Effect of atmosphere on the mechanical milling of natural graphite. *Carbon* 38(15):2077–2085
- Hu C, Liu ACY, Weyland M, Madani SH, Pendleton P, Rodríguez-Reinoso F, Kaneko K, Biggs MJ (2015) A multi-method study of the transformation of the carbonaceous skeleton of a polymer-based nanoporous carbon along the activation pathway. *Carbon* 85:119–134
- Kobayashi T, Sumiya K, Fukuba Y, Fujie M, Takahagi T, Tashiro K (2011) Structural heterogeneity and stress distribution in carbon fiber monofilament as revealed by synchrotron micro-beam X-ray scattering and micro-Raman spectral measurements. *Carbon* 49(5):1646–1652
- Montes-Morán MA, Young RJ (2002) Raman spectroscopy study of HM carbon fibres: effect of plasma treatment on the interfacial properties of single fibre/epoxy composites. *Carbon* 40(6):845–855

34. Cuesta A, Dhamelincourt P, Laureyns J, Martínez-Alonso A, Tascón JMD (1998) Effect of various treatments on carbon fiber surfaces studied by Raman microprobe spectrometry. *Appl Spectrosc* 52(3):356–360
35. Samuel BA, Rajagopalan R, Foley HC, Haque MA (2010) Effect of pyrolysis temperature on the microstructure of disordered carbon nanowires. *Thin Solid Films* 519(1):91–95
36. Goncalves ES, Rezende MC, Ferreira NG (2006) Dynamics of defects and surface structure formation in reticulated vitreous carbon. *Braz J Phys* 36(2a):264–266
37. Barros EB, Demir NS, Souza Filho AG, Mendes Filho J, Jorio A, Dresselhaus G, Dresselhaus MS (2005) Raman spectroscopy of graphitic foams. *Phys Rev B: Condens Matter Mater Phys* 71:1–5
38. Baldan MR, Almeida EC, Azevedo AF, Gonçalves ES, Rezende MC, Ferreira NG (2007) Raman validity for crystallite size La determination on reticulated vitreous carbon with different graphitization index. *Appl Surf Sci* 254:600–603
39. Couzi M, Bruneel JL, Talaga D, Bokobza L (2016) A multi wavelength Raman scattering study of defective graphitic carbon materials: the first order Raman spectra revisited. *Carbon* 107:388–394
40. Chernyak SA, Ivanov AS, Maslakov KI, Egorov AV, Shen Z, Savilov SS, Lunin VV (2017) Oxidation, defunctionalization and catalyst life cycle of carbon nanotubes: a Raman spectroscopy view. *Phys Chem Chem Phys* 19(3):2276–2285
41. Yi Y, Weinberg G, Prenzel M, Greiner M, Heumann S, Becker S, Schlögl R (2017) Electrochemical corrosion of a glassy carbon electrode. *Catal Today* 295:32–40
42. Hu C, Sedghi S, Silvestre-Albero A, Andersson GG, Sharma A, Pendleton P, Rodríguez-Reinoso F, Kaneko K, Biggs MJ (2015) Raman spectroscopy study of the transformation of the carbonaceous skeleton of a polymer-based nanoporous carbon along the thermal annealing pathway. *Carbon* 85:147–158
43. Frackowiak E, Francóis B (2001) Carbon materials for the electrochemical storage of energy in capacitors. *Carbon* 39(6):937–950
44. Chen XL, Li WS, Tan CL, Li W, Wu YZ (2008) Improvement in electrochemical capacitance of carbon materials by nitric acid treatment. *J Power Sources* 184(2):668–674
45. Zou Y, Wang S (2015) Interconnecting carbon fibers with the in-situ electrochemically exfoliated graphene as advanced binder-free electrode materials for flexible supercapacitor. *Sci Rep* 5:1–7
46. Stoller MD, Ruoff RS (2010) Best practice methods for determining an electrode material's performance for ultracapacitors. *Energy Environ Sci* 3(9):1294
47. Venkatesh S, Vishista K (2018) Identification of the best chemical equivalent ratio to produce emeraldine salt exhibiting better pseudo capacitance. *Electrochim Acta* 263:76–84
48. Ra EJ, Raymundo-Piñero E, Lee YH, Béguin F (2009) High power supercapacitors using polyacrylonitrile-based carbon nanofiber paper. *Carbon* 47(13):2984–2992
49. Nian Y-R, Teng H (2002) Nitric acid modification of activated carbon electrodes for improvement of electrochemical capacitance. *J Electrochem Soc* 149(8):A1008
50. Momma T, Liu X, Osaka T, Ushio Y, Sawada Y (1996) Electrochemical modification of active carbon fiber electrode and its application to double-layer capacitor. *J Power Sources* 60(2): 249–253
51. Kim WJ, Ko TH, Seo MK, Chung YS, Kim HY, Kim BS (2018) Engineered carbon fiber papers as flexible binder-free electrodes for high-performance capacitive energy storage. *J Ind Eng Chem* 59: 277–285
52. Díez N, Díaz P, Álvarez P, González Z, Granda M, Blanco C, Santamaría R, Menéndez R (2014) Activated carbon fibers prepared directly from stabilized fibers for use as electrodes in supercapacitors. *Mater Lett* 136:214–217
53. Hsieh CT, Teng H (2002) Influence of oxygen treatment on electric double-layer capacitance of activated carbon fabrics. *Carbon* 40(5): 667–674
54. Sivakkumar SR, Kim WJ, Choi JA, MacFarlane DR, Forsyth M, Kim DW (2007) Electrochemical performance of polyaniline nanofibres and polyaniline/multi-walled carbon nanotube composite as an electrode material for aqueous redox supercapacitors. *J Power Sources* 171(2):1062–1068
55. Shang X, Chi J-Q, Lu S-S, Gou J-X, Dong B, Li X, Liu Y-R, Yan K-L, Chai Y-M, Liu C-G (2017) Carbon fiber cloth supported interwoven WS₂ nanoplates with highly enhanced performances for supercapacitors. *Appl Surf Sci* 392:708–714
56. Li C, Wang D, Wang X, Liang J (2005) Controlled electrochemical oxidation for enhancing the capacitance of carbon nanotube composites. *Carbon* 43(7):1557–1560